VERTICAL ARRANGEMENT AND WAVEFUNCTION CONTROL IN STRUCTURES WITH 2D QUANTUM DOTS

I.L. KRESTNIKOV[a], M. STRASSBURG, M. CAESAR, V.A. SHCHUKIN[a], A. HOFFMANN, U.W. POHL AND D. BIMBERG

Technische Universität Berlin, Hardenbergstraße 36, Berlin D-10623, Germany
E-mail: igor@sol.physik.tu-berlin.de

N.N. LEDENTSOV, V.G. MALYSHKIN, P.S. KOP'EV AND ZH.I. ALFEROV

A.F.Ioffe Physical-Technical Institute, St.Petersburg 194021, Russia

D. LITVINOV, A. ROSENAUER AND D. GERTHSEN

Laboratorium für Elektronenmikroskopie der Universität Karlsruhe, 76128 Germany

Exciton wavefunction engineering in arrays of two-dimensional (2D) quantum dots (QDs) is considered on the example of nanoscale islands formed using ultrathin (submonolayer or 1 ML) CdSe insertions in a ZnSe matrix. Vertical stacking of sheets of islands separated by ZnSe layers results in two basic vertical arrangements: vertical correlation or anticorrelation, as it follows from both experimental investigations and the theory of growth. In these two types of vertically ordered QD structures the electronic spectrum is drastically different, resulting in different optical transition energies and different polarization of edge emission. QD exciton-induced resonant waveguiding and lasing are observed for both types of QD states.

1 Introduction

Recently, much attention is attracted to the investigations of the low-dimensional structures: quantum wires (QWWs) and quantum dots (QDs), fabricated using self-organized growth approaches [1]. The most important problem for these kinds of nanostructures is to provide a possibility to control the geometry and the uniformity of QWWs and QDs to govern their electronic spectra. In this work we offer a principally new way to design such objects by using differently vertically-arranged two-dimensional (2D) islands. Uniform 2D QDs are formed in our case using ultrathin (submonolayer or 1 monolayer) narrow gap CdSe insertions [2] in a wide gap ZnSe matrix. The driving force for the formation of arrays of uniform in size 2D islands on the crystal surface during submonolayer deposition originates from different intrinsic surface stress tensors for the deposit and the substrate. The elastic relaxation of the surface phase with higher surface stress value makes formation of boundaries favorable. On the other hand, additional dangling bonds formed at the

[a] On leave from Ioffe Institute

island edges do not let the island size to be too small. Both effect taken together are resulting in an equilibrium size of the 2D islands [3]. The total energy of surface array of islands, which can be written:

$$E_{SURF} = -\frac{\alpha}{L}\ln(\beta L) + \frac{\gamma}{L}, \qquad (1),$$

where α and β are coefficients accounting for the difference in intrinsic surface stress between two phases and γ shows the role of the short-range potential due to additional dangling bonds formed at the island edges. The equilibrium size of the island (L_0) is determined by the minimum of Eq. (1) which exists at *any* finite positive values of coefficients α, β and γ. In contrast, for homoepitaxial submonolayer deposition $\alpha = 0$, and the minimum energy corresponds to an infinite island size, meaning continuous ripening of *2D* islands. For 2D islands having above 1 ML height one needs to include in Eq. 1 an additional term due to elastic strain relaxation related to possible lattice mismatch between the substrate and the deposit [4]. This term is important for 2D islands formed by 1 ML and slightly above 1 ML deposition.

As opposite to three-dimensional QDs, in the 2D case the volume of the potential well is rather small resulting in relatively small QD exciton localization energies with respect to the matrix bandgap energy. Thus, a very important task existing for these QDs is to find a way of increasing of the localization energy and, more generally, in achieving higher degree of wavefunction control without increase in the inhomogeneity of the system. This can be potentially done by stacking of sheets of 2D islands in the vertical direction. In this case, however, the islands formed during the each next depositions cycle grow in different conditions as compared to the single-cycle deposition, as their formation occurs in the strain field created by the buried islands of the previous sheets. The arrangement of the islands in the upper sheet reaches the equilibrium under the constraint of the fixed structure of buried islands which affect energy balance via creating a potential profile on the surface.

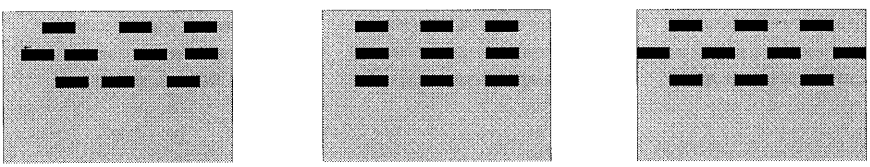

Figure 1. Different possibilities of vertical ordering for structures with multi-sheet arrays of 2D islands: no correlation (a), vertical correlation (b) and anticorrelation (c).

Three basic possibilities of vertical arrangement of islands depicted in Fig. 1a-c can be realized: no correlation, vertical correlation and vertical anticorrelation, respectively. In the case of very thick spacers or small lattice mismatch between the substrate and the deposit, the influence of the underlying insertions is minor, and no correlation can be expected (Fig.1a). For the case of strong lattice distortions there can be two main possibilities for vertical arrangement: vertical correlation, when the islands in the successive sheets are placed directly above the islands in the preceding sheet (Fig. 1b), and vertical anticorrelation when the islands in the upper sheet are placed above the separating regions in the previous sheet (Fig.1c).

In this work we study submonolayer (SML) and one-monolayer (ML) CdSe insertions in a ZnSe matrix. We demonstrate the possibility of both vertically correlated and anticorrelated ordering of stacked CdSe/ZnSe 2D QDs. A close interconnection between the type of ordering and the electronic spectrum is revealed.

2 Experimental

2.1 Sample growth

The structures studied in this work are grown on n+ GaAs(100) substrates using molecular beam epitaxy (MBE) at a substrate temperature of 280°C [5]. All structures consist of 360 nm ZnSSe buffer and 60 nm ZnSSe cap layers lattice matched to the GaAs substrate. Between these layers a CdSe/ZnSe SML SL is inserted. The average thickness of a single CdSe insertion is estimated as 0.7 ML. ZnSe barriers separate the sheets of CdSe SML insertions and have thicknesses of 15 Å, 30 Å, 50 Å and 80 Å. The total thickness of the SML SL region is 60 nm for the structures with 30 Å, 50 Å and 80 Å barriers and 30 nm for the structure with 15 Å barriers. Consequently, the numbers of SL periods is different (20, 20, 12 and 8 for 15 Å, 30 Å, 50 Å and 80 Å barriers, respectively). The thickness of the buffer layer corresponds to only a few photon wavelengths in the crystal. For this geometry the optical confinement of the light wave due to the *average* refractive index change between the active SML SL and the passive $ZnS_{0.06}Se_{0.94}$ cladding layers is negligible, and the emitted light should be effectively absorbed by the GaAs substrate if no compensating resonant waveguiding effects are available.

2.2 Optical and structural characterization

The investigated II-VI SML SLs were characterized using photoluminescence (PL), optical reflectance (OR), and photoluminescence excitation (PLE) spectroscopy. For studies at high excitation densities a pulsed dye laser pumped by an excimer laser is used. The same system was used for PLE measurements.

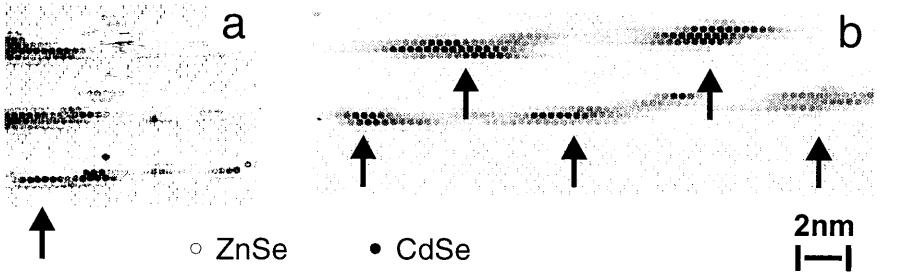

Figure 2. Different possibilities of vertical ordering for structures with multi-sheet arrays of 2D islands: no correlation (a), vertical correlation (b) and anticorrelation (c).

Cross-section high-resolution electron microscopy (HREM) is performed along the <110> direction using a PHILIPS CM 200 FEG/ST electron microscope with a Scherzer resolution of 0.24 nm. To reveal the distribution of the strained cadmium selenide insertions, digitized HREM images are processed by the evaluation program DALI that allows the determination of *local* lattice parameters (LLP).

3 Structural characterization and growth theory

HREM studies revealed that SML or 1 ML CdSe insertions in a ZnSe matrix result in formation of uniform islands having lateral sizes of 40-50 Å and an average CdSe thickness in the island region of 1 – 2 MLs [6, 7]. For thin (15 Å) spacer thickness the vertical correlation was demonstrated [8]. When the spacer thickness is increased up to 30 Å a mixed situation with some vertically correlated (Fig. 2a), but predominantly anticorrelated (Fig. 2b) islands is observed [7, 8]. To treat the system quantitatively we have developed a growth model, which is based on the following main assumptions:

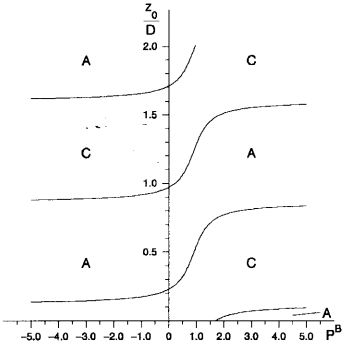

Figure 3. The model phase diagram of elastic interaction between the array of surface islands and the array of buried islands. P^B is the anisotropy of double force density of buried islands. z_0 is the separation between sheets of the surface and the buried islands, and D is the in-plane period. C denotes vertical correlation, and A denotes vertical anticorrelation.

1. We consider 2D islands of 1-2 ML height having a fixed lateral size, where the tunable parameter is the ratio of the separation between successive sheets with 2D islands and the lateral periodicity of the islands on the surface.
2. Elastic anisotropy of the cubic crystal is included.

The elastic anisotropy is known to favor ordering of nanostructures in elastically soft directions and

one can expect a significant effect of elastic anisotropy on vertical correlation between islands.

Since the cubic crystals with zinc-blend structure have a negative parameter of elastic anisotropy:

$$\xi = \frac{c_{11} - c_{12} - 2c_{44}}{c_{44}} < 0, \qquad (2)$$

where c_{11}, c_{12} and c_{44} are elastic moduli of a cubic crystal in the Voigt notation, an oscillatory decay of the strain produced by buried islands is possible. It can result in the alternation of vertical correlation and anticorrelation with spacer thickness between successive sheets of islands [9]. Fig.3 shows a calculated phase diagram for arrays of 2D islands. P^B is a parameter describing the ratio of the forces created by Cd atom in a *2D* CdSe 1 ML insertion in the directions perpendicular and parallel to the interface. This parameter P_B is believed to be close to unity for the CdSe/ZnSe system, while some finite deviation may originate from different environment of the Cd atom in the insertion for in-plane and vertical directions. The exact percent of the deviation can be calculated from the first principles model and is not discussed here. One can see from Fig. 2b that the alternation of vertically correlated to anticorrelation growth with z_0 occurs for vertical periodicity of the structure below $0.5D$ assuming P_B=1. The in-plane period for our structures evaluated from the HREM data is 100 Å. Thus, the transition from correlated to anticorrelated growth should occur at spacer thickness below 50 Å. The HREM data gives the transition thickness of 30 Å in our case, in a very good agreement with theory, and pointing that the exact P_B value is close to 0.6.

4 Electronic properties

Different vertical arrangements of islands must result in different electronic spectra of structures which consist of short period SML superlattices (SLs). To confirm this prediction we performed optical characterization of the structures. PL spectra of SML SLs having different spacer layer thickness (d_{sp}) are shown in Fig. 4. For large d_{sp} only one line is observed. The transition energy corresponds to heavy hole-like QD excitons localized at the two-dimensional nanoscale islands with lateral extensions comparable to the exciton radii in ZnSe. At d_{sp} equal to 30 Å, a second lower energy luminescence line evolves. Despite the low energy PL line dominates the spectrum, OR data indicates

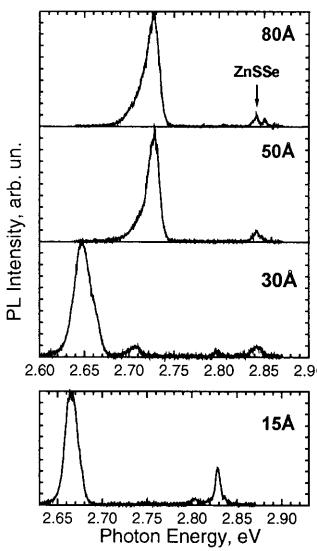

Figure 4. Photoluminescence (PL) spectra of samples with different thicknesses of the ZnSe spacer layers.

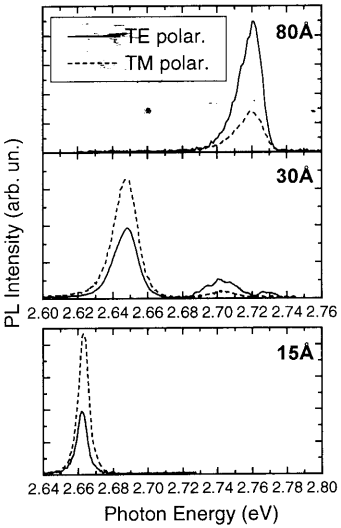

Figure 5. Linearly polarized spectra of edge emission for structures with 80 Å, 30 Å and 15 Å spacers. (T = 7 K, P_{exc}= 3 W/cm^2, E_{exc}= 3.81 eV).

that the concentration of the corresponding states is relatively low and the OR resonance corresponds to the remaining higher energy line. Finally, for d_{sp}=15 Å the lower energy feature completely dominates both in PL and OR spectra. On the basis of the HREM data and the growth model discussed above one may conclude that the appearance of the second line is related to vertically-correlated growth of 2D islands. The vertical correlation of the islands results in an efficient coupling of electronic states of vertically neighboring QDs. Exciton wavefunction expands in vertical direction through the chain of closely coupled quantum dots, and the role of size quantization in z-direction diminishes.

Vertical expansion of the wavefunction must affect the polarization of the edge PL of SML SLs. It is well known, that in a quantum well (QW) case, the heavy-hole exciton emission is completely TE polarized in edge geometry, according to the Kane's selection rules. The polarized PL spectra of the structures with 80 Å, 30 Å, and 15 Å spacers, measured at edge geometry, are shown in Fig. 5. One can conclude that the emission of well-separated uncoupled QDs is predominantly TE polarized, in agreement with much stronger *k*-quantization in z-direction for ultrathin 2D islands. However, in the structure d_{sp} =30 Å, the polarization of the second low-energy line related to the coupled QDs is reversed to predominantly TM. This observation clearly indicates the expansion of the heavy hole exciton wavefunction in the growth direction. The higher energy line due to anticorrelated QDs remains predominantly TE polarized. In the sample with 15 Å spacers, where correlated islands completely dominate, only the TM-polarized emission is observed. Thus, our results clearly demonstrate a new possibility to engineer QD exciton wavefunctions using the correlated and the anticorrelated growth of 2D islands and provide unique possibilities for polarization control of edge-emitting devices.

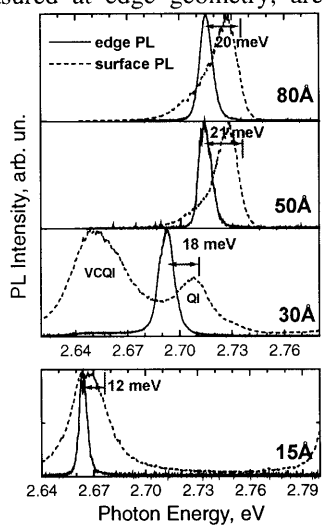

Figure 6. Edge and surface PL of structures with different spacer layer thickness (T_{reg}= 7 K, P_{exc}=100 kW/cm^2, E_{exc}= 2.88 eV).

5 Resonant waveguiding and lasing in stacked 2D quantum dots

The principal advantage of the SML SLs composed of dense arrays of two-dimensional nanoscale islands is the possibility to achieve ultrahigh absorption or gain values and realize an intrinsic resonant waveguiding effect (excitonic waveguide) without using of thick cladding layers having a lower refractive index [6]. The effect is based on a resonant enhancement of the refractive index in the vicinity of the exciton resonance in accordance with the Kramers-Kronig equations. Since the studied structures are grown on thin buffer layers placed directly on strongly absorbing GaAs substrates, the resonant modulation of the refractive index must be remarkably strong to provide resonant waveguiding and to reduce the absorption losses related to the GaAs substrate. This is possible because of the ultrahigh material absorption/gain in values QDs and the remarkably high density of 2D islands for stacked SML insertions. Another strict requirement to enable excitonic waveguiding is the lifting of the *in plane* k-selection rule, which prohibits zero-phonon emission of excitons with finite kinetic energy that dominate at high temperatures or excitation densities in II-VI bulk-like and in QW structures. In the latter structures, the phonon-assisted gain mechanism dominates, which occurs in the spectral range downshifted from the photon energy range of efficient resonant waveguiding. The in-plane k-selection rule is not appropriate in QDs, and the zero-phonon gain resonant to the resonant waveguiding spectral region becomes possible [6]. No need in thick cladding layers having a lower *average* refractive indices exists in this case [10].

A comparison of the surface PL at high excitation densities and stimulated emission recorded from the edge of the structure is shown in Fig. 5. The energies of the transitions corresponding to the QD ground states, revealed in the OR spectra of the structures, are shown by solid segments. The stimulated emission originates from uncoupled QDs structures with larger spacer layer thickness and is revealed by strong superlinear growth of intensity with excitation density and narrowing of the PL line. The stimulated emission from coupled QD is observed only in case of the 15 Å spacers where the density of the coupled states becomes high. The zero-phonon nature of the QD emission is confirmed by the energy positions of the stimulated emission and the gain maximum. The red shift of the stimulated emission is distinctly smaller than the LO-phonon energy, proving the zero-phonon gain mechanism both for correlated and anticorrelated QD structures. The energy position of the gain maximum does not shift with the excitation density manifesting excitonic nature of the gain mechanism, which is manifested up to room temperature [11].

Conclusions and acknowledgments

A possibility of tuning of vertical arrangement is shown theoretically and experimentally for structures with 2D islands formed by SML- or 1ML- depositions. A new possibility to control effectively the electronic spectrum of 2D QDs, the localization energies of excitons confined at 2D islands, and the polarization of edge PL is demonstrated. Resonant waveguiding and lasing is observed for both types of vertical arrangement of 2D QDs.

We are grateful to Dr. S.V. Ivanov and Dr. S.V. Sorokin for the growth of the samples. This work was supported by the RFBR, the Program of "Physics of solid-states nanostructures" and DFG. I.L.K. and N.N.L. are grateful to the DFG and to the Alexander von Humboldt Foundation, respectively.

References

1. N.N. Ledentsov, *Prog. Crystal Growth and Charact.*, **35**, 289 (1997).
2. M. Strassburg, V. Kutzer, U.W. Pohl, A. Hoffmann, I. Broser, N.N. Ledentsov, D. Bimberg, A. Rosenauer, U. Fischer, D. Gerthsen, I.L. Krestnikov, M.V. Maximov, P.S. Kop'ev, Zh.I. Alferov, *Appl. Phys. Lett.*, **72**, 942 (1998).
3. V.I. Marchenko, *JETP lett.*, **33**, 381 (1981).
4. J. Tersoff, and R.M. Tromp, *Phys.Rev.Lett.*, **70**, 2782 (1993).
5. S.V. Ivanov, A.A. Toropov, T.V. Shubina, S.V. Sorokin, A.V. Lebedev, I.V. Sedova, P.S. Kop'ev, G.R. Pozina, J.P. Bergman, B. Monemar, *J. Appl. Phys.*, **83**, 3168 (1998).
6. N.N. Ledentsov, I.L. Krestnikov, M.V. Maximov, S.V. Ivanov, S.V. Sorokin, P.S. Kop'ev, Zh.I. Alferov, D. Bimberg, C.M. Sotomayor Torres, *Appl. Phys. Lett.*, **69**, 1343 (1996), *ibid* **70**, 2888 (1997).
7. M. Strassburg, V. Kutzer, U.W. Pohl, A. Hoffmann, I. Broser, N.N. Ledentsov, D. Bimberg, A. Rosenauer, U. Fischer, D. Gerthsen, I.L. Krestninov, M.V. Maximov, P.S. Kop'ev, Zh.I. Alferov, *Appl. Phys. Lett.*, **72**, 942 (1998).
8. I.L. Krestninov, M. Strassburg, M. Caesar, A. Hoffmann, U.W. Pohl, D. Bimberg, N.N. Ledentsov, P.S. Kop'ev, Zh.I. Alferov, D. Litvinov, A. Rosenauer, D. Gerthsen, *Phys. Rev. B, will be published.*
9. V.A. Shchukin, D. Bimberg, V.G. Malyshkin, N.N. Ledentsov, *Phys. Rev. B*, **57**, 12262 (1998).
10. A.V. Sakharov, S.V. Ivanov, S.V. Sorokin, I.L. Krestnikov, B.V. Volovik, N.N. Ledentsov, P.S. Kop'ev, *Technical Physics Letters*, **23**, 305 (1997).
11. I.L. Krestnikov, M.V. Maximov, A.V. Sakharov, P.S. Kop'ev, Zh.I. Alferov, N.N. Ledentsov, D. Bimberg, C.M. Sotomayor Torres, *J.Cryst. Growth*, **184/185**, 545 (1998).

III. HETEROSTRUCTURES AND SUPERLATTICES: OPTICAL